Available online at www.sciencedirect.com
ScienceDirect
Electrochimica Acta 52 (2007) 5985–5996
ELECTROCHIMICA Acta
www.elsevier.com/locate/electacta

Separation and concentration effect of *f*-MWCNTs on electrocatalytic responses of ascorbic acid, dopamine and uric acid at *f*-MWCNTs incorporated with poly (neutral red) composite films

Umasankar Yogeswaran, Shen-Ming Chen *,[1]

Department of Chemical Engineering and Biotechnology, National Taipei University of Technology, No.1, Section 3, Chung-Hsiao East Road, Taipei 106, Taiwan

Received 15 October 2006; received in revised form 25 February 2007; accepted 19 March 2007
Available online 24 March 2007

Abstract

A novel conductive composite film containing functionalized multi-walled carbon nanotubes (*f*-MWCNTs) with poly (neutral red) (PNR) was synthesized on glassy carbon electrodes (GC) by potentiostatic method. The composite film exhibited promising electrocatalytic oxidation of mixture of biochemical compounds such as ascorbic acid (AA), dopamine (DA) and uric acid (UA) in pH 4.0 aqueous solutions. It was also produced on gold electrodes by using electrochemical quartz crystal microbalance technique, which revealed that the functional properties of composite film were enhanced because of the presence of both *f*-MWCNTs and PNR. The surface morphology of the polymer and composite film deposited on transparent semiconductor tin oxide electrodes were studied using scanning electron microscopy and atomic force microscopy. These two techniques showed that the PNR was fibrous and incorporated on *f*-MWCNTs. The electrocatalytic responses of neurotransmitters at composite films were measured using both cyclic voltammetry (CV) and differential pulse voltammetry (DPV). These experiments revealed that the difference in *f*-MWCNTs loading present in the composite film affected the electrocatalysis in such a way, that higher the loading showed an enhanced electrocatalytic activity. From further electrocatalysis studies, well separated voltammetric peaks were obtained at the composite film modified GC for AA, DA and UA with the peak separation of 0.17 V between AA–DA and 0.15 V between DA–UA. The sensitivity of the composite film towards AA, DA and UA in DPV technique was found to be 0.028, 0.146 and 0.084 $\mu A\ \mu M^{-1}$, respectively.

Keywords: Functionalized multiwall carbon nanotubes; Composite film modified electrodes; Electrocatalysis; Vitamin C; Dopamine; Uric acid

1. Introduction

Electrochemically functional polymer films and carbon nanotubes (CNTs) films have been of great interest for the past decade in the electrocatalysis reactions because of their unique chemical and electrochemical properties. Previous studies demonstrated conjugated polymers showing interesting electrocatalytic activities such as, reduction of acetylene in poly-3-methylthiophene, reduction of dioxygen at 4,4′,4″,4‴-tetraaminophthalocyanine macrocycles, oxidation of glucose by polypyrrole and oxidation of NADH, reduction of IO_3^-, BrO_3^- at poly (neutral red) (PNR) films [1–4]. On the other hand, CNTs have shown interesting electrocatalytic activities for both bioorganic and inorganic compounds such as glutathione, homocysteine, carbohydrates, NADH, nitric acid, hydrogen peroxide, etc. [5–12]. In addition CNTs were also used for methanol oxidation in the fuel cells, detection of insulin and oxidation of acetic acid. Their wide varieties of applications have developed a great interest in the electrocatalysis field [13–15]. Even though the electrocatalytic activity of the CNTs and conjugated polymer films were individually good, some properties like mechanical stability, sensitivity for different techniques and electrocatalysis for multiple compounds were not efficient. So, new studies have been developed in the past decade for the preparation of the composite films, which are composed of both CNTs and conducting polymers with enhanced electrocatalytic activity [16–18].

The rolled-up graphene sheets of carbon, i.e., CNTs exhibit a π-conjugative structure with a highly hydrophobic surface.

* Corresponding author. Tel.: +886 2270 17147; fax: +886 2270 25238.
E-mail address: smchen78@ms15.hinet.net (S.-M. Chen).
[1] ISE Member.

0013-4686/$ – see front matter © 2007 Elsevier Ltd. All rights reserved.
doi:10.1016/j.electacta.2007.03.047

This unique property of the CNTs allows them to interact with some organic aromatic compounds through π–π electronic and hydrophobic interactions to form new structures [19–21]. These interactions were used for preparing composite sandwiched films for electrocatalytic studies such as selective detection of dopamine in the presence of ascorbic acid [22] and in the designing of nano devices with the help of non-covalent adsorption of enzyme and proteins on the side walls of CNTs. This resulted in a novel CNTs based nanostructures, which contain biochemical units in them [23]. The electrodeposition of CNTs with polypyrrole composite films too was studied in detail [24]. Electrodes modified with composite films were widely used in capacitors, battery and material science, photo electrochemistry, fuel cells, chemical sensors and biosensors [25,26].

Ascorbic acid (AA) being a constituent of the cell has momentous biological functions and is an analyte of great importance. It is found in fruits, vegetables and in beverages especially those derived from fruit juices [28], which mainly act as a preventer of respiratory viral infections [29]. Dopamine (DA) is one of the most important neurotransmitters in the central nervous system of the mammals, which exist in the tissues and body fluids in the form of cations for controlling the nervous system [30]. Uric acid (UA) and other oxypurines are the principal final products of purine metabolism in the human body [31]. Abnormal levels of UA cause symptoms of several diseases, including gout, hyperuricemia and Lesch-Nyan disease [32]. However AA, DA and UA coexist in biological fluids such as blood and urine. Due to their crucial role in neurochemistry and industrial applications, several traditional methods have been used for their determination. Among those, electrochemical methods have more advantage over the other because; in these the electrodes sense the neurotransmitters, which are present with in the living organisms [27]. Electrochemical analysis on the unmodified electrodes, for example glassy carbon has limitations because of the overlapping of oxidation potentials of AA, DA and UA and hence often suffers from a pronounced fouling effect that results in rather a poor selectivity and reproducibility [33,34]. For electrochemical analysis, multilayer films of shortened negatively-charged multiwalled carbon nanotubes (MWCNTs) were homogeneously and stably assembled on glassy carbon (GC) electrodes by layer-by-layer (LBL) method using electrostatic interaction of positively-charged poly(diallyldimethylammonium chloride) (PDDA) [22]. In the past, several modified electrodes were used for the simultaneous determination of AA and DA [35,36], specifically PNR modified electrodes too were used [37]. Further, the simultaneous determination of AA and UA were also reported [38].

The electropolymerization of neutral red (NR) from aqueous solution and its catalytic activity towards biomolecules and different inorganic compounds were already reported. The structure of the neutral red monomer ($C_{15}H_{17}N_4^+$) and the possible composition of the PNR film showing the tetramer were in the Scheme 1(a) and (b), respectively [39]. Further the literature survey reveals that previously there were no attempts made for the synthesis of composite film using CNTs with PNR. In this article, we report a novel composite film

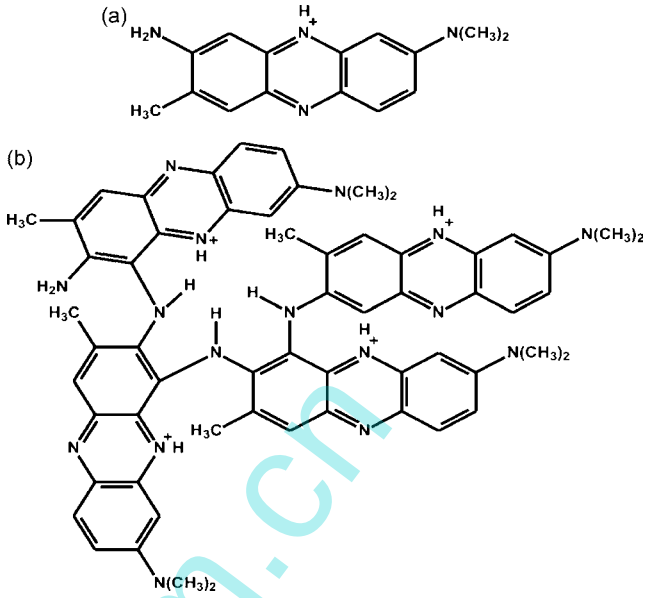

Scheme 1. (a) Structure of neutral red monomer ($C_{15}H_{17}N_4^+$) and (b) possible composition of the PNR film showing the tetramer.

(*f*-MWCNTs-PNR) made of functionalized mutiwall carbon nanotubes (*f*-MWCNTs) incorporated with PNR, along with its characterization. Different concentration effects of *f*-MWCNTs in the composite film, the composite film's enhancement in functional properties, film stability, peak current and electrocatalytic activity are also reported. Not only limited to these, we also report its application on effective separation of biochemical compounds such as AA, DA and UA, even at very wide concentrations. The film formation process involved the modification of glassy carbon electrode (GC) with uniform well dispersed *f*-MWCNTs aqueous solution and then electropolymerization of the neutral red from neutral aqueous solution on the *f*-MWCNTs modified GC.

2. Experimental

2.1. Apparatus

Cyclic voltammetry (CV) and differential pulse voltammetry (DPV) were performed in an analytical system model CHI-400 and CHI-900 potentiostat, respectively. A conventional three-electrode cell assembly consisting of an Ag/AgCl reference electrode and a platinum wire counter electrode was used for electrochemical measurements. The working electrode was either an unmodified glassy carbon electrode or a glassy carbon electrode modified with the *f*-MWCNTs-PNR films. In this, all the potentials were reported versus the Ag/AgCl reference electrode. The working electrode for EQCM measurements was an 8 MHz AT-cut quartz crystal coated with a gold electrode. The diameter of the quartz crystal was 13.7 mm; the gold electrode diameter was 5 mm. The morphological characterizations of *f*-MWCNTs-PNR composite films were examined by means of scanning electron microscopy (SEM) (Hitachi S-3000H) and atomic force microscopy (AFM) (Being Nano-Instruments CSPM4000).

2.2. Materials

Neutral red (NR) and multiwall carbon nanotubes (MWCNTs OD = 10–20 nm, ID = 2–10 nm and length = 0.5–200 μm) were obtained from Aldrich. All other chemicals used were of analytical grade. The preparation of aqueous solutions was done with twice distilled deionized water. Freshly prepared solutions of ascorbic acid, dopamine and uric acid were used for all the experiments. Solutions were deoxygenated by purging with pre-purified nitrogen gas. Buffer solutions were prepared from H_2SO_4 and KHP (potassium hydrogen phthalate) aqueous buffer for the pH 1.0 and 4.0, respectively. All experiments were carried out at room temperature (i.e., 25 °C ± 2).

2.3. Preparation of f-MWCNTs and f-MWCNTs-PNR modified GCs

There was an important challenge in the preparation of *f*-MWCNTs. Because of its hydrophobic nature, it was difficult to disperse it in any aqueous solution to get a homogeneous mixture. Briefly, the hydrophobic nature of the MWCNTs was converted in to hydrophilic nature by following the previous studies [16]. This was done by weighing 10 mg of MWCNTs and 200 mg of potassium hydroxide in to a ruby mortar and ground together for 2 h at room temperature. Then the reaction mixture was dissolved in 10 mL of double distilled deionized water then precipitated many times in to methanol for the removal of potassium hydroxide. Then the obtained MWCNT-OHs (*f*-MWCNTs) in 10 mL water were ultrasonicated for 6 h to get homogeneous dispersion.

Before starting each experiment, the glassy carbon electrode was polished by a BAS polishing kit with 0.05 μm alumina slurry, rinsed and was ultrasonicated in double distilled deionized water. Four types of films were studied from uniformly coated *f*-MWCNTs at different concentrations, 0 μg cm^{-2} (PNR), 2.1 μg cm^{-2} (composite-1), 6.4 μg cm^{-2} (composite-2) and 12.8 μg cm^{-2} (composite-3). Then the electropolymerization of NR (5×10^{-5} M) on *f*-MWCNTs modified GCs was done by electrochemical oxidation of NR in pH 4.0, 1.0 M KHP buffer solution. It was performed by consecutive CV over a suitable potential range of (0.9 to −0.5 V) for pH 4.0 and (1.0 to −0.4 V) for pH 1.0 aqueous solutions; number of cycles for all the experiments was 20. The electrolyte used for pH 1.0 was H_2SO_4 aqueous solution. The fifth type of electrode studied was 12.8 μg cm^{-2} of *f*-MWCNTs on GC without PNR (*f*-MWCNTs). The different concentrations of homogeneously dispersed *f*-MWCNTs were exactly measured using micro-syringe then coated on the GC surface and dried at about 40 °C.

3. Results and discussions

3.1. Electrochemical preparation and characterization of PNR and f-MWCNTs-PNR composite films

The electropolymerization of NR (5×10^{-5} M) by electrochemical oxidation on the *f*-MWCNTs modified GC in aqueous solutions (pH 1.0 and 4.0) were preformed for preparing different kinds of *f*-MWCNTs-PNR composite films. The growth of the CV current in Fig. 1(A) corresponds to two redox couples of PNR in pH 4.0, the formal potentials were $E^{\circ\prime} = -0.35$ and 0.2 V versus Ag/AgCl. In this, the $E^{\circ\prime}$ at −0.35 V represents redox reaction of monomer and oligomer formed during the electropolymerization. The $E^{\circ\prime}$ at 0.2 V represents the redox reaction of oligomer and polymer [40]. Fig. 1(B) shows the electropolymerization of NR (5×10^{-5} M) on composite-3 film modified GC in pH 4.0, 1.0 M KHP buffer solution, where there was a huge increment in the electropolymerizing current when comparing PNR film. Fig. 1(C) shows the comparison of the CVs of GC with (a) PNR; (b) composite-1; (c) composite-2 and (d) composite-3 films at similar conditions; here all four films showed the same formal potential for electropolymerization. However, there was an increase in peak currents for both the redox couples when increasing the *f*-MWCNTs loading. These results clearly differentiated between the polymer and the three kinds of composite films. Further the formed films were characterized using electrochemical and microscopic methods such as CVs, weighing method in quartz crystal microbalance, SEM, AFM, etc. The PNR surface coverage concentrations (Γ) for different loads of *f*-MWCNTs were listed in Table 1, these values clearly indi-

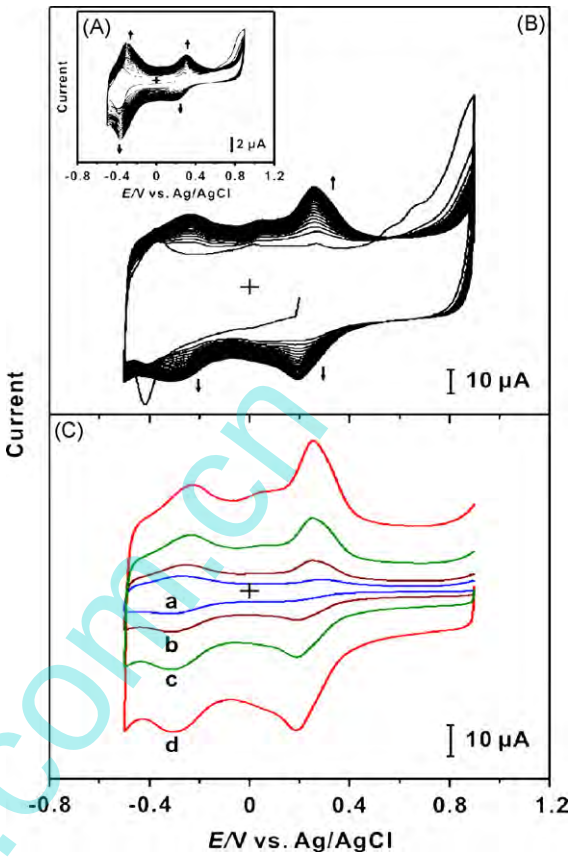

Fig. 1. Repetitive CVs of GC (A) modified from 5×10^{-5} M NR in 0.1 M KHP buffer pH 4.0 aqueous solution, scan rate at 100 mVs^{-1}; (B) composite-3 film at similar conditions; (C) CVs of (a) PNR; (b) composite-1; (c) composite-2 and (d) composite-3 films at similar conditions, here the peak current and calculated values (Table 1) reveals the increase in Γ of PNR when increasing *f*-MWCNTs loading.

Table 1
Surface coverage concentrations of PNR on different modified electrodes for different techniques in 0.1 M KHP buffer pH 4.0 aqueous solution

Technique	NR[a] (M)	Type of film	(Γ)[b] of PNR (mol cm^{-2})
CV[c]	5×10^{-5}	PNR	9.49×10^{-12}
		Composite-1	1.26×10^{-11}
		Composite-2	1.97×10^{-11}
		Composite-3	3.13×10^{-11}
EQCM[d]	5×10^{-4}	PNR	2.43×10^{-11}
		f-MWCNTs-PNR	7.85×10^{-11}

[a] Concentration of NR in the 0.1 M KHP buffer pH 4.0 aqueous solution.
[b] (Γ) represents surface coverage concentration.
[c] GC electrode was used for CV technique.
[d] Quartz crystal coated with gold electrode was used for EQCM technique.

cated that, increase in concentration of *f*-MWCNTs on GC leads to the increase in Γ of PNR deposited on the electrode. These results too showed that, the increase in surface area of electrode occurred due to the increase in *f*-MWCNTs loading. The plots in Fig. 2(A–D) were the electrochemical properties of PNR and composite-3 films at different scan rates (up to 500 mVs^{-1}) in the potential range of 0.8 to −0.5 V (CV figures not shown). These CVs were carried out in pH 4.0 of 0.1 M KHP buffer aqueous solution in the absence of NR. The anodic and cathodic peak currents in Fig. 2(A) of the PNR film and the composite-3 film redox couples increased linearly with the increase of scan rates. But the peak currents in Fig. 2(B) increased slower than the square root of scan rate until 300 mVs^{-1}, indicating that the redox process was surface controlled until 300 mVs^{-1} for composite-3 film. Similarly, Fig. 2(C) reveals that the redox process of PNR film was diffusion limited for above 220 mVs^{-1} scan rates. The inset in Fig. 2(D) is the comparison of peak separations of redox couple ($E^{\circ\prime} = 0.2$ V) for the PNR and composite-3 films, here the peak separation for composite-3 was lower than PNR until 300 mVs^{-1}. This result indicates that the electron transfer rate for composite-3 film was higher than that of PNR film. This was evident from the calculated values of electron transfer rate (*K*s) using the Eq. (1) based on Laviron theory [41].

$$\log Ks = \alpha \log(1-\alpha) + (1-\alpha)\log\alpha - \log\left(\frac{RT}{nF\upsilon}\right) - \frac{\alpha(1-\alpha)nF\Delta E}{2.3RT} \quad (1)$$

By assuming α as 0.5 (from the slopes in Fig. 2(D)) and the number of electrons and protons involved as two [42,43], the *K*s for PNR and composite-3 films were calculated as 0.142 s^{-1} (±0.005) and 0.109 s^{-1} (±0.002), respectively. In this, the scan rate and ΔE values are in unit volts. The percentage of increase in the electron transfer rate in the presence of *f*-MWCNTs in composite film was 30.5%. Fig. 2(E) shows the CVs of composite-3 film in various pH aqueous buffer solutions, where the electropolymerization of the composite film was done in pH 1.0 aqueous buffer solution. These showed that the film was stable in pH range between 1 and 13 and the values of $E^{\circ\prime}$ (−0.35 and 0.2 V) depends on the pH value of the buffer solution.

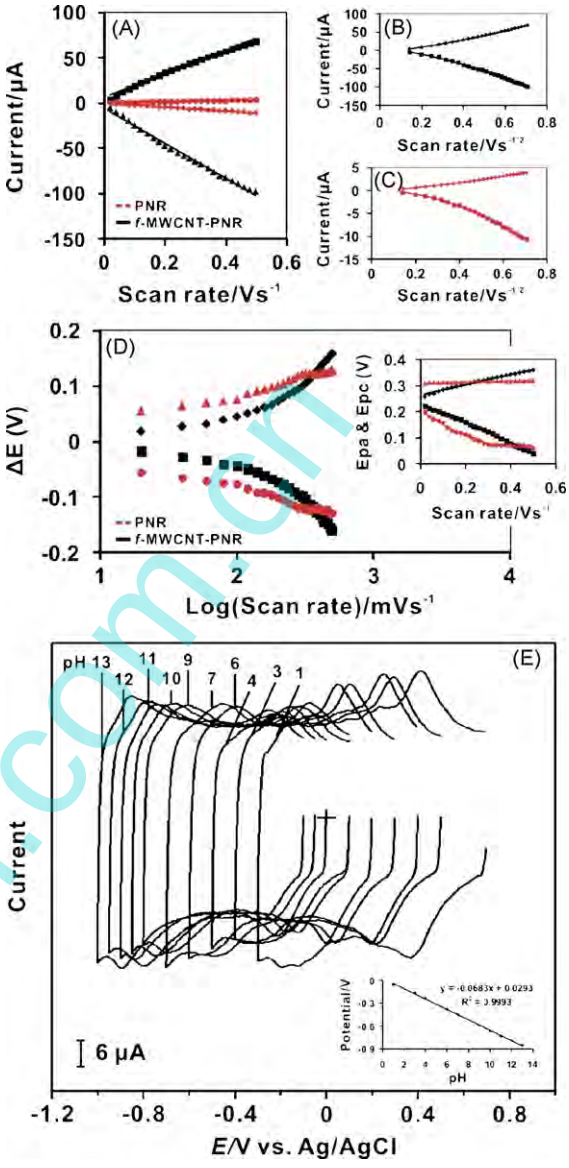

Fig. 2. (A) Shows the plot of peak currents ($E^{\circ\prime} = 0.2$ V) of both PNR and composite-3 film vs. scan rate (up to 500 mVs^{-1}). The plots in (B) PNR and (C) composite-3 film were peak current vs. square root of scan rate. These three figures revealed that both the films were not diffusion controlled until 220 mVs^{-1} for PNR and 300 mVs^{-1} for composite-3 films. (D) Shows a plot of ΔE vs. log of scan rate and the inset in (D) shows the plot of Epa and Epc vs. scan rate for both the films, from these results it was clear that the electron transfer rate was higher for composite-3 film comparing PNR. (C) CVs of the composite-3 film synthesized at pH 1.0 on GC and transferred to various pH solutions. The inset shows the formal potential vs. pH, the slope −68 mV/pH almost nearer to Nernstian equation.

The pH dependent $E^{\circ\prime}$ value reveals that, redox couples of the composite-3 film include some proton transfer during the redox reactions. The inset in Fig. 2(E) shows, the formal potential of composite-3 film plotted over a pH range of 1 to 13 with a slope of −68 mV/pH. This value was close to that given by the Nernstian equation, for two electrons and two protons involved in the redox reaction. These results are similar to the previously reported literatures for PNR [42,43].

The electrochemical quartz crystal microbalance (EQCM) experiments were carried out by modifying the gold coated quartz crystals, with a minimum concentration of uniformly coated *f*-MWCNTs and dried at 40 °C. It was carefully done to avoid the over deposition of *f*-MWCNTs, which could cause the crystal to be inactive. The maximum concentration of *f*-MWCNTs could be deposited before the inactivation of the crystal was found to be 0.61 μg cm^{-2}. On the other hand, the concentration of the NR was also optimized according to the surface activity of the EQCM gold electrode; only at 5×10^{-4} M NR there was an obvious decrease in frequency noted for the polymer growth. The concentration below 5×10^{-4} M NR does not show any frequency change for the polymer growth. Fig. 3(A) shows the consecutive CVs and electrochemical quartz crystal microbalance (EQCM) results for the PNR film from the solution containing 5×10^{-4} M NR. Fig. 3(B) indicates the change in the EQCM frequency recorded during the cycles of the consecutive CV. The increase in the voltammetric peak current of PNR redox couple in Fig. 3(A) and the frequency decrease (or mass increase) in Fig. 3(B) were found to be consistent with the growth of the PNR film on the gold electrode. Fig. 3(E) shows the consecutive CVs and electrochemical quartz crystal microbalance (EQCM) results for the *f*-MWCNTs-PNR composite from the solution containing 5×10^{-4} M NR. Fig. 3(F) indicates the change in the EQCM frequency recorded during the cycles of the consecutive CV. The increase in the voltammetric peak current of composite redox couple in Fig. 3(E) and the frequency decrease (or mass increase) in Fig. 3(F) were found to be consistent with the growth of the PNR film on the *f*-MWCNTs modified gold electrode. These results too showed that the obvious deposition potential that was started between +0.9 and −0.5 V. From the frequency change, the change in the mass in composite film at the quartz crystal can be calculated by the Sawerbery equation. However, 1 Hz frequency change was equivalent to 1.4 ng of mass change [44,45]. The mass change during PNR incorporation on the gold electrode and *f*-MWCNTs modified gold electrode for total cycles was found to be 728 ng cm^{-2} and 374 ng cm^{-2}, respectively. However, the values of Γ in Table 1 for EQCM shows an increase in Γ of PNR on *f*-MWCNTs modified electrode than on the bare gold electrode. This major contradiction between both the values (mass change and Γ) could be because of the instability of *f*-MWCNTs during first 5–6 cycles of electropolymerization on the gold electrode. Comparing the frequency change in Fig. 3(B) and (F) we noticed that the deposition of PNR was higher up to 6 cycles for unmodified electrode and then followed by much un-stabilized deposition. But on *f*-MWCNTs modified electrode highly stabilized deposition of PNR taken place after 6 cycles. The relatively large electrodeposition for the first 6 cycles shows the more adherence property of PNR to the electrode surface. This also proves that the *f*-MWCNTs stability on the gold electrode increased because of PNR deposition. Fig. 3(C and G) indicates the variation of (a) cathodic peak current with the increase of the scan cycles and (b) every cycle of cathodic peak

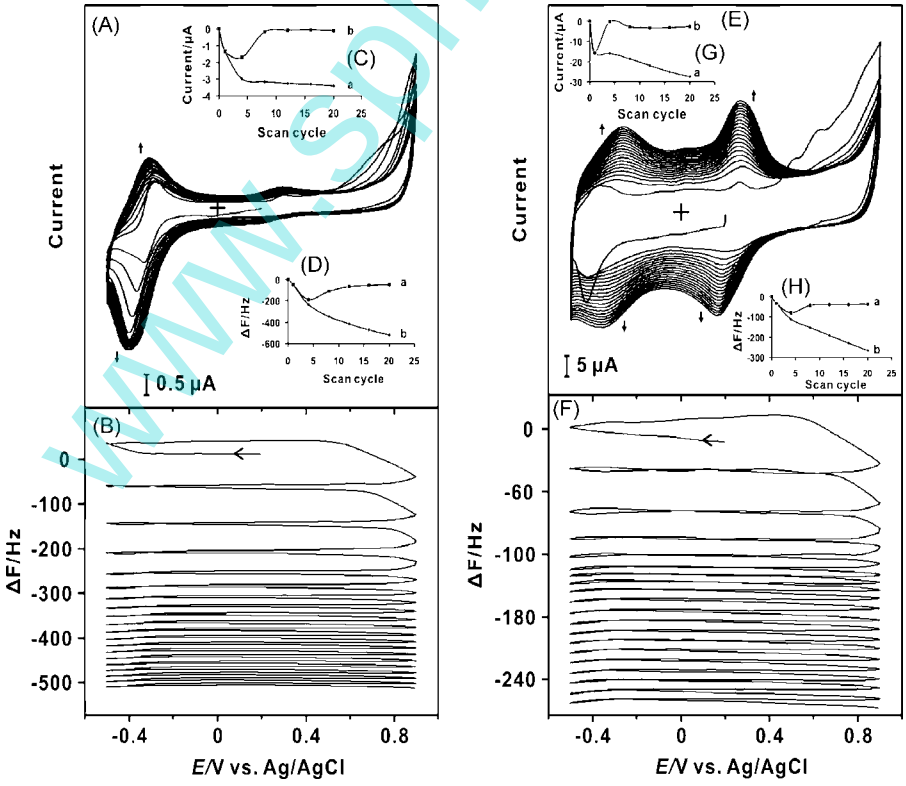

Fig. 3. Consecutive potential CVs of a gold electrode modified from (A) 5×10^{-4} M NR and (E) composite-3 in 0.1 M KHP buffer pH 4.0 aqueous solution. (B) and (F) are the EQCM frequency change responses recorded together with the consecutive CVs between +0.9 and −0.5 V, scan rate: 20 mVs^{-1}. (C) and (G) (a) Plot of cathodic peak current vs. scan cycle; (b) every cycle of cathodic current change vs. scan cycle. (D) and (H) (a) Every cycle frequency change Δf vs. scan cycle; (b) total frequency change Δf vs. scan cycle. These results show the composite was a stabilized one and more homogeneously deposited.

current with the increase of the scan cycles. Fig. 3(D and H) indicates the variation of (a) every cycle frequency change with the increase of scan cycles and (b) frequency change with the increase of the scan cycles. Fig. 3(C and G)(a) and Fig. 3(D and H)(b) were found to be consistent with a linear change in the growth of PNR film on the gold electrode and *f*-MWCNTs modified gold electrode, respectively. Also there was only one redox couple for PNR film and two redox couples for the *f*-MWCNTs-PNR composite film on the gold electrode. This clearly shows the formation of the composite film. From these EQCM results we could conclude that the deposition of the *f*-MWCNTs-PNR composite film was more stabilized and more homogeneous and the PNR plays an important role in the stability of the *f*-MWCNTs on the electrode surface. Similar previous studies on CNTs-polymer composites showed the necessity of the polymer on the carbon nanotubes for improving the functional properties such as orientation, enhanced electron transport (higher conductivity), high capacitance, etc. [46,47].

Further, the PNR and the *f*-MWCNTs-PNR composite films were prepared on the indium tin oxide (ITO) with similar conditions and similar potential as that of GC and were characterized using the SEM and AFM techniques. The top SEM views of nano structures in Fig. 4(A) PNR (5×10^{-5} M) on the ITO electrode shows PNR was formed as fibrous structures on the surface; (B) *f*-MWCNTs-PNR on the ITO electrode shows *f*-MWCNTs with PNR an obvious formation of composite film. The topographic images obtained from AFM Fig. 4(C) PNR (5×10^{-5} M) on the ITO electrode shows PNR was formed as globular and fibrous structures on the surface similar to SEM result; (D) shows *f*-MWCNTs-PNR on the ITO electrode. In a large area point of view (in nano scale $\approx$ 13000 nm) the surface of *f*-MWCNTs-PNR was uneven comparing to that of PNR film. So the tip deflection to generate the root mean square amplitude (RMS) value in tapping mode AFM measurement was not enough for graphing the *f*-MWCNTs-PNR surface amplitude. Because of these complications the large scale measurement was not possible and not equivalent to PNR film measurement. However, here we reduced the area of measurement so that the surface would be more evenly scanned. From these images we can clearly identify the difference between both the films formed on ITO. Further, Fig. 4(E and F) shows the three-dimensional AFM images of the same modified ITO electrodes.

3.2. Electrocatalytic oxidation of AA, DA and UA at the *f*-MWCNTs-PNR film modified electrodes

The CVs of the electrochemical oxidation of AA, DA and UA at different film modified and unmodified electrodes were

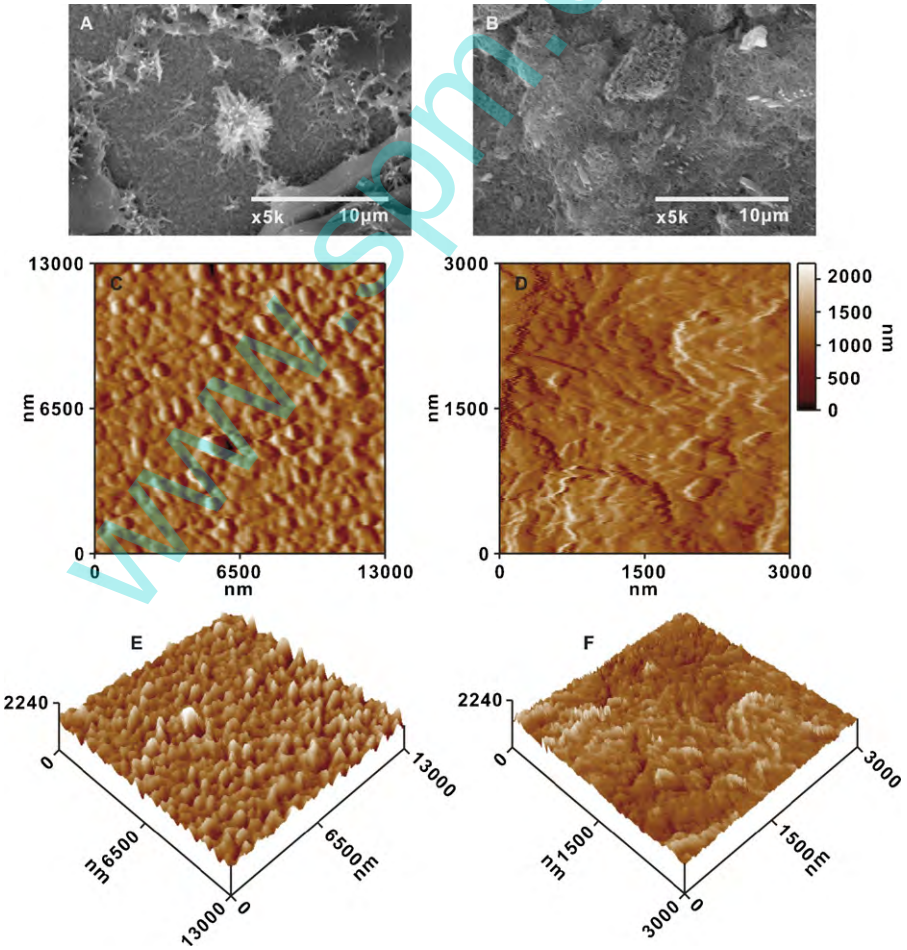

Fig. 4. SEM images of (A) PNR and (B) *f*-MWCNTs-PNR composite films. AFM and its 3D images of (C and E) were PNR and (D and F) were *f*-MWCNTs-PNR composite films. These show the obvious formation of composite film.

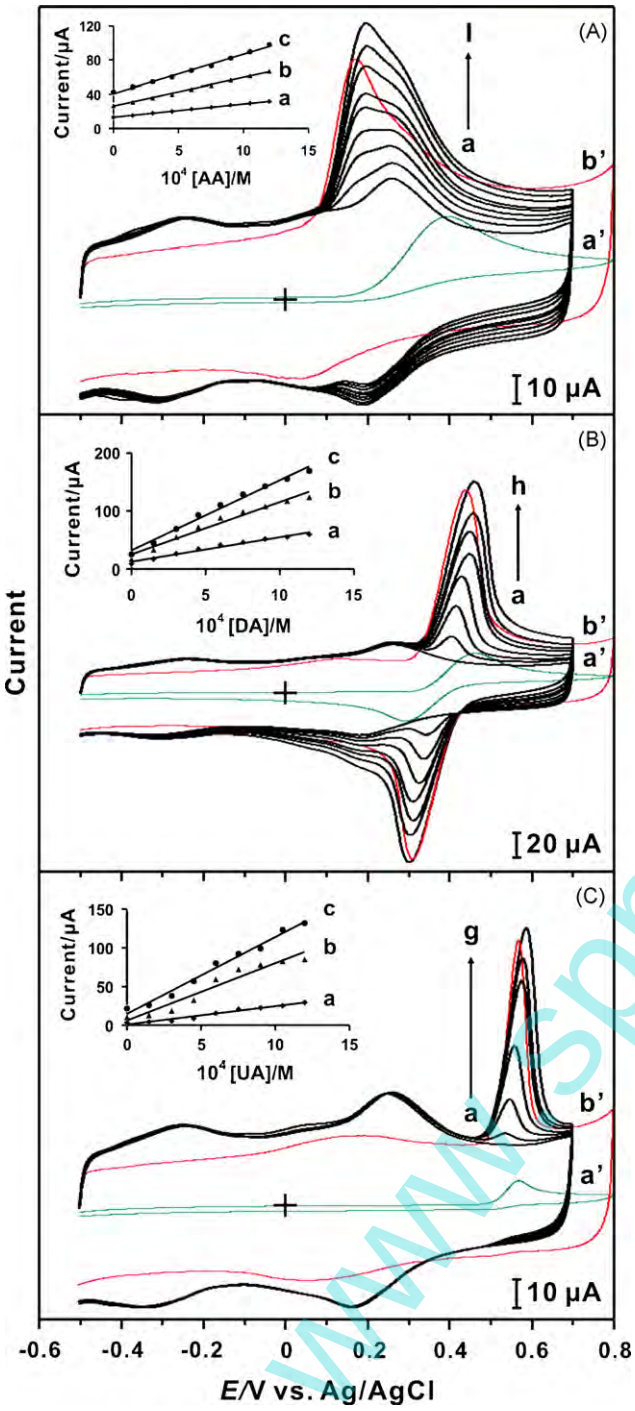

Fig. 5. CVs of the composite-3 film in 0.1 M KHP buffer pH 4.0 aqueous solution with various concentration of (A) AA = (a) 0.0; (b) 1.5×10^{-4}; (c) 3×10^{-4}; (d) 4.5×10^{-4}; (e) 6×10^{-4}; (f) 7.5×10^{-4}M; (g) 9×10^{-4}; (h) 1.05×10^{-3} and (i) 1.2×10^{-3} M. (B) DA = (a) 0.0; (b) $1.5x10^{-4}$; (c) $3x10^{-4}$; (d) 4.5×10^{-4}; (e) 6×10^{-4}; (f) 7.5×10^{-4}; (g) 9×10^{-4}; (h) 1.2×10^{-3} M. (C) UA = (a) 0.0; (b) 1.5×10^{-4}; (c) 3×10^{-4}; (d) 4.5×10^{-4}; (e) 7.5×10^{-4}; (f) 9×10^{-4} and (g) 1.2×10^{-3} M. Where (a′) and (b′) represents bare GC and only *f*-MWCNTs, respectively, in the highest concentration of the analytes. The insets in (A); (B) and (C) shows the plot of current vs. different concentration of AA, DA and UA, respectively with: (a) composite-1; (b) composite-2 and (c) composite-3 films.

shown in Fig. 5. In all these figures (a′) represents electrocatalysis at bare GC electrode and (b′) represented at *f*-MWCNTs modified GC with similar conditions to that of composite-3 film. The electrolyte used for all the following electrocatalysis experiments was pH 4.0 KHP buffer solution. The CVs exhibited a reversible redox couple for composite-3 film in the absence of AA. Upon the addition of AA, a new oxidation peak of AA similar to the anodic peak potential of composite-3 redox couple was appeared at Epa = 0.25 V. An increase in the concentration of AA (a–i) simultaneously produced an increase in the oxidation current of AA with good film stability. Another observation was, from 0.45 mM AA a new peak (Epa = 0.19 V) appeared and the peak (Epa = 0.25 V) diminished. Comparison of this result with that of b′ (Epa = 0.17 V) reveals that the appearance of new peak was because of the electrocatalytic activity of *f*-MWCNTs present in the composite film towards the analyte. Also, b′ showed lower overpotential than composite-3 film. However, the electrocatalytic peak current of b′ was smaller than AA oxidation at composite-3 (Table 2). Fig. 5(B) shows the CVs of the electrochemical oxidation of DA at composite-3 film. The CVs exhibited a reversible redox couple for composite-3 film in the absence of DA. Upon the addition of DA, a new growth in the oxidation peak of DA appeared at Epa = 0.46 V. An increase in the concentration of DA (a–h) simultaneously produced an increase in the oxidation current of DA with good film stability. Comparison of electrocatalytic activity of *f*-MWCNTs and composite-3 film reveals that b′ has lower overpotential, but with lower peak current, which was similar to AA. In Fig. 5(C) the electrochemically active film of composite-3 was deposited on GC and performed the electrocatalytic oxidation of UA. Here (a–g) represents six different concentrations of UA at composite-3 film; (b′) represents *f*-MWCNTs modified GC and (a′) represents bare GC electrode at similar conditions. The CVs exhibited a reversible redox couple for composite-3 film in the absence of UA. Upon the addition of UA, a new growth in the oxidation

Table 2
Comparison of Epa and Ipa for AA, DA and UA using CV technique on different types of modified electrodes in 0.1 M KHP buffer pH 4.0 aqueous solution

Analytes	Electrode type	Epa (V)	Ipa (μA)
AA (Oxidation)	Bare GC	0.40	29.38
	PNR	0.65	16.70
	Only *f*-MWCNTs	0.17	84.99
	Composite-1	0.23	31.40
	Composite-2	0.22	67.08
	Composite-3	0.19	97.97
DA (Oxidation)	Bare GC	0.46	31.88
	PNR	0.72	19.80
	Only *f*-MWCNTs	0.44	161.3
	Composite-1	0.41	59.77
	Composite-2	0.43	124.0
	Composite-3	0.45	169.3
UA (Oxidation)	Bare GC	0.57	91.82
	PNR	0.72	5.124
	Only *f*-MWCNTs	0.56	93.78
	Composite-1	0.56	29.13
	Composite-2	0.58	85.74
	Composite-3	0.61	112.0

peak of UA appeared at Epa = 0.61 V. An increase in the concentration of UA simultaneously produced an increase in the oxidation current of UA with good film stability. Comparing these results it was clear that (b′) showed reduced overpotential, but with lower peak current as given in Table 2. The general electrocatalytic oxidation reaction of AA, DA and UA at the electrode surface could be represented by the Scheme 2(a, b and c), respectively [48,49]. The insets in Fig. 5(A, B and C) represents the current of AA, DA and UA respectively versus the concentration of each analyte, which showed the effect of different concentrations of *f*-MWCNTs on the each analyte's oxidation peak current, where *a* = composite-1, *b* = composite-2 and *c* = composite-3. When comparing these insets with that of Ipa values in Table 2 we can clearly note the increase in electrocatalytic peak currents due to the increase of *f*-MWCNTs concentration present in the composite film.

The concentration effects of *f*-MWCNTs and PNR on electrocatalysis (lower overpotential) for individual analytes can be explained from Table 2. In this, all the three analytes showed that bare GC and PNR modified electrodes has similar Epa. But for composite-3 film, the Epa of all analytes showed lower overpotential. However, the composite film modified electrodes have different effects on each analytes as given below. The oxidation of AA at the higher concentration of *f*-MWCNTs composite film shows lower overpotential. Controversially, (b′) shows less positive potential peak when comparing all the composite films. This was because of the adsorption of AA on the high surface area of *f*-MWCNTs. Moreover, it was a well known fact that at pH 4, less molar fractions of ascorbate anion exists, so the interaction with positively charged PNR film and negatively charged ascorbate anion will be very low. This can also be a reason for the higher positive potential shift of AA at composite films, when comparing only *f*-MWCNTs modified GC. Then, the oxidation of DA at the different concentrations of *f*-MWCNTs was almost similar. However, in high concentrations of *f*-MWCNTs, DA has higher positive peak potential shift when comparing with other composite films. This could be explained by the increase in peak current, which makes the DA oxidation in to a quasi reversible reaction with peak shifting. This reveals that, the DA oxidation could be more efficient with more recovery on composite-1 film rather than the other films. The insoluble nature of UA enhances its adsorption on *f*-MWCNTs, thus (b′) have lower overpotential for UA than the composite films. Anyhow, all the three analytes do not show much difference in potential shift related to concentration effect of *f*-MWCNTs. But there were higher peak currents for all three analytes noted when *f*-MWCNTs concentration increased at the composite film. Finally, these Ipa and Epa observations clearly state that the enhancement in the peak current and lower overpotential for all the three analytes at the composite were due to the presence of *f*-MWCNTs. From the literature, by comparing polymer [37] and CNTs [50,51] modified electrodes, it is inferred that the CNTs-polymer composite film modified electrodes exhibited enhanced catalytic activity with excellent functional properties. This was due to the presence of both CNTs and polymer, where the CNTs enhanced the electrocatalytic activity and the polymer provided the film stability with excellent functional properties [46,47]. This was similar to our above presented results, where PNR shows excellent functional properties (EQCM) such as enhancement in *f*-MWCNTs adhesion on the electrode surface. Then, the *f*-MWCNTs enhanced the electrocatalytic activity (CVs) of the composite film.

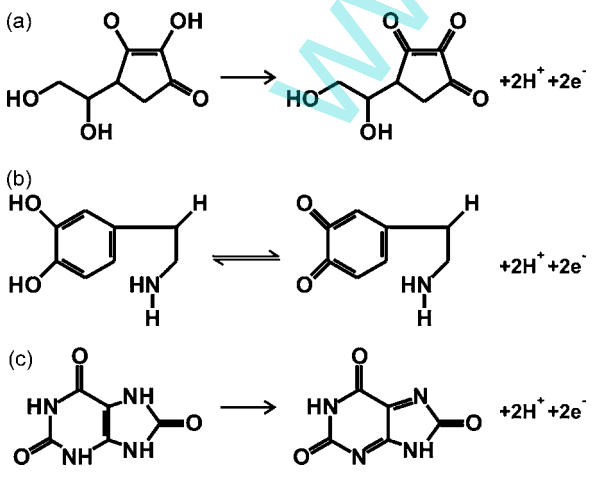

Scheme 2. Electrocatalytic oxidation of (a) AA; (b) DA and (c) UA at *f*-MWCNTs-PNR film modified electrodes.

3.3. Voltammeric resolution of AA with DA and UA at PNR, *f*-MWCNTs and *f*-MWCNTs -PNR film modified electrodes

Fig. 6(A–C) depicts the cyclic voltammograms that were obtained for AA, DA and UA coexisting (AADAUA) in pH 4.0 KHP aqueous buffer solution at the PNR, *f*-MWCNTs, composite-3 film modified GCs and (a′) bare GC. The cyclic voltammogram on bare GC (a′) in Fig. 6(A–C) exhibited with one broad peak and another peak with less difference in peak potential (0.10 V) for AADAUA mixture. Here, the broad peak represents the voltammetric signals of AA and DA and the second peak represents the voltammetric signals of UA. Moreover, the peak current decreased in the subsequent cycles. These observations clearly indicated that the bare glassy carbon electrode failed to separate the voltammetric signals of AA, DA and UA in a mixture. The fouling effect of the electrode surface with the oxidized products of AA and DA were the reasons for obtaining the weak single peak for AA, DA and UA mixture [52]. The electroactive PNR film Fig. 6(A) also did not show any peak separation for the three analytes, the sluggish reaction kinetics with fouling effect and no Ipa increase higher than (a′), all these cause the failure to separate the peak potentials of the three analytes. Fig. 6(B) and (C) shows the CVs of the electrochemical oxidation of eight different concentrations (a–i) of AADAUA mixture at only *f*-MWCNTs and composite-3 respectively (Epa values in Table 3). From these two figures, it is clear that, the peak separation of AA and DA on only *f*-MWCNTs was higher than that of composite films, which can be explained as the adsorption of AA on the high surface area of *f*-MWCNTs. In Fig. 6(C) the CVs exhibited a reversible redox couple for composite-3 films in the absence of AADAUA mixture. Upon the addition of AADAUA, three new growths in the oxidation peak for AA, DA and UA were appeared. An increase in the concentration of AADAUA mixture simultaneously produced an increase in the oxidation

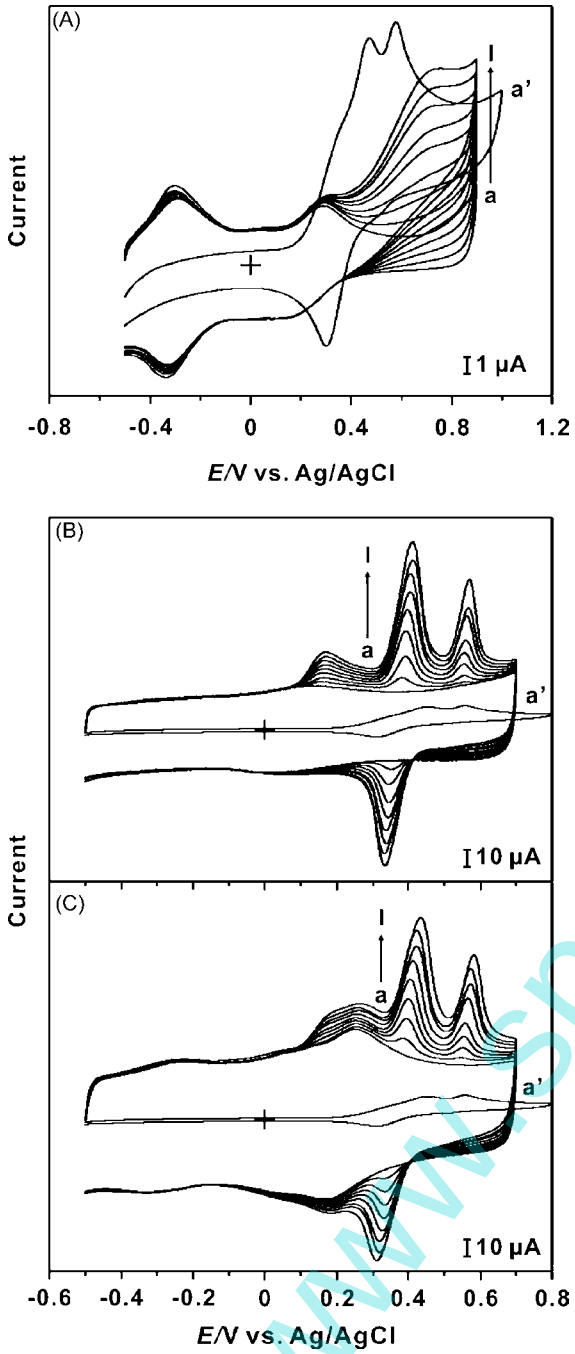

Fig. 6. CVs of the (A) PNR; (B) only *f*-MWCNTs and (C) composite-3 film in 0.1 M KHP buffer pH 4.0 aqueous solution with various individual concentrations of AA, DA and UA mixture (represented by AADAUA): (a′) bare GC and [AADAUA] = 3×10^{-4} M; [AADAUA] = (a) 0.0; (b) 3.75×10^{-5}; (c) 7.5×10^{-5}; (d) 1.125×10^{-4}; (e) 1.5×10^{-4}; (f) 1.875×10^{-4}; (g) 2.25×10^{-4}; (h) 2.625×10^{-4} and (i) 3×10^{-4} M.

current of AA, DA and UA with good film stability. The obvious peak separation between the analytes in composite-3 film were because of the electrostatic and hydrophobic interaction between the three analytes with the fixed cationic sites on PNR ($pK_a = 6.8$) [53] and also the negatively charged fixed sites on *f*-MWCNTs. The Scheme 3 shows the interactions of all the three analytes at the *f*-MWCNTs-PNR composite modified in the pH 4.0 KHP buffer electrode, which involves a two electron and

Table 3
Peak separation of AA, DA and UA in a mixture of all three analytes, using CV technique on different types of electrodes in 0.1 M KHP buffer pH 4.0 aqueous solution

Electrode type	AA (Epa in V)	DA (Epa in V)	UA (Epa in V)	AA–DA[a] (V)	DA–UA[b] (V)
Bare GC	0.45	0.45	0.55	–	0.10
PNR	0.72	0.72	0.72	–	–
Only *f*-MWCNTs	0.17	0.41	0.56	0.24	0.15
Composite-1	0.24	0.38	0.56	0.14	0.18
Composite-2	0.24	0.39	0.56	0.15	0.17
Composite-3	0.26	0.43	0.58	0.17	0.15

[a] Peak separation of AA and DA in the mixture.
[b] Peak separation of DA and UA in the mixture.

two proton process [42,48,49]. This too shows the redox reaction, which was involved for PNR, during the electrocatalysis of analytes at composite film. Further, the difference in the concentration of *f*-MWCNTs on the composite film too affected the peak separation as shown in Table 3, where AA and DA peak separation increased because of the increase in concentration of *f*-MWCNTs. On the other hand, the DA and UA peak separation decreased. Comparing the Fig. 5 (A) and Fig. 6 (C) we confirmed also that the appearance of two oxidation peaks for AA was, one because of the PNR and the other because of *f*-MWCNTs.

Fig. 7 shows the plot of individual concentrations of AA (a), DA (b) and UA (c) in the mixture versus current at (A) composite-1; (B) composite-2 and (C) composite-3 film modified GC electrodes. From these graphs it was clear that by increasing the concentration of *f*-MWCNTs, more increase in electrocatalytic peak current of DA occurred when comparing to that of AA and UA. This was because of the higher diffusion rate of the DA [54]. It can be explained as the electrostatic attractive effect between the positively charged DA species and the negatively charged fixed sites on the *f*-MWCNTs [16], which facilitated the faster diffusion of the DA in to the *f*-MWCNTs-PNR composite film. The results based on this concept in Fig. 5(B) with Fig. 7 graphs were concordant. Also, we could see the overall current increase in CV because of the increase in *f*-MWCNTs concentration. So, this plays an important role in sensitivity in the detection of different analytes.

3.4. The differential pulse voltammograms of AA with DA and UA at f-MWCNTs-PNR film modified electrodes

Fig. 8(A) shows the differential pulse voltammograms (DPV) which were obtained during the simultaneous change of the concentrations of AADAUA mixture at composite-3 film modified electrode. The DPVs were recorded at a constant time interval of 2 min with nitrogen purging before the start of each experiment. They demonstrated that the calibration curves for AA, DA and UA were linear for a wide range of concentrations from 0.075 to 0.2 mM. These were one of the widest concentrations used for the detection of AA, DA or UA in aqueous solution [50,51]. The slopes of the linear calibration curves between the peak current and the concentration were estimated as 0.028, 0.146 and

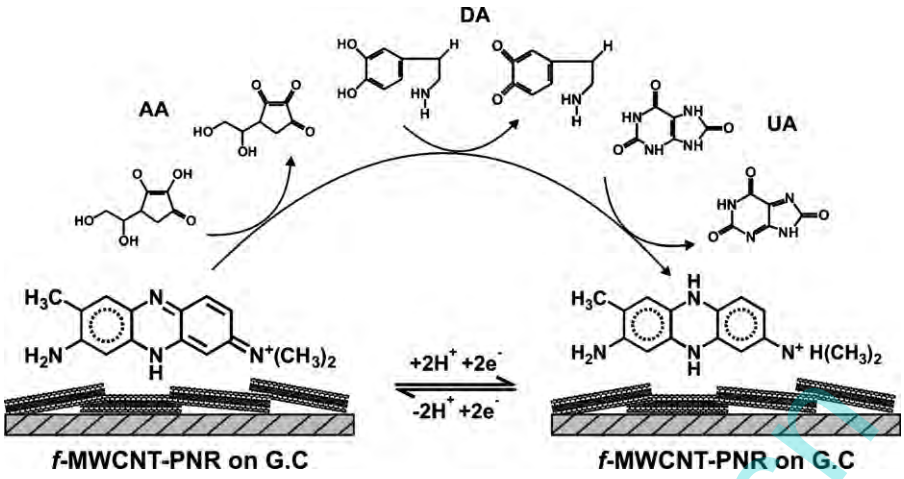

Scheme 3. Different interactions of AA, DA and UA at *f*-MWCNTs-PNR composite modified electrode.

0.084 μA μM^{-1} for AA, DA and UA, respectively. The correlation co-efficient of the slopes for AA, DA and UA were found 0.900, 0.995 and 0.987, respectively. Interestingly, the peak currents for DA and UA were higher when comparing AA, this phenomenon occurred due to the reason that the diffusion of DA and UA through the composite film was much faster compared to that of AA [54]. Also, the AA oxidation peak has two peaks, one because of the activity of PNR and the other because of *f*-MWCNTs; these were similar to the CV results. Fig. 8(B) shows the DPV of the simultaneous change in concentrations of AADAUA mixture at *f*-MWCNTs modified electrode without PNR. The calibration curves of all the analytes were not linear; the interactions between the three analytes were high and complicated for each addition of concentration. For the oxidation of AA there appears only a broad peak. This result clearly shows that, only *f*-MWCNTs modified GC electrode was not suitable for the DPV technique. This was because of the reduced hydrophobic interaction in the *f*-MWCNTs, which is due to its preparation methods [16].

Fig. 8(C) exhibits the DPVs that were obtained for the different concentrations of DA and UA (a–e) in the presence of 20 mM concentration of AA at composite-3 film modified electrode. The ratio of AA with DA and UA was 266:1, which was higher than the previously reported ratios [49,50]. The voltammetric peak corresponding to the oxidation of DA and UA was found increased linearly in consonance with the increase of the bulk concentration of DA and UA whereas the peak current for oxidation of AA slightly got decreased as the number of cycles increased. This was due to the UA accumulation on sidewalls; the accumulation takes place because of its less solubility and high adsorption nature. Inset in Fig. 8(C) shows that the calibration plots for DA and UA were linear with a slope of 0.099 and 0.159 μA μM^{-1}; and the correlation co-efficient of DA and UA was found to be 0.923 and 0.908. By comparing the slope

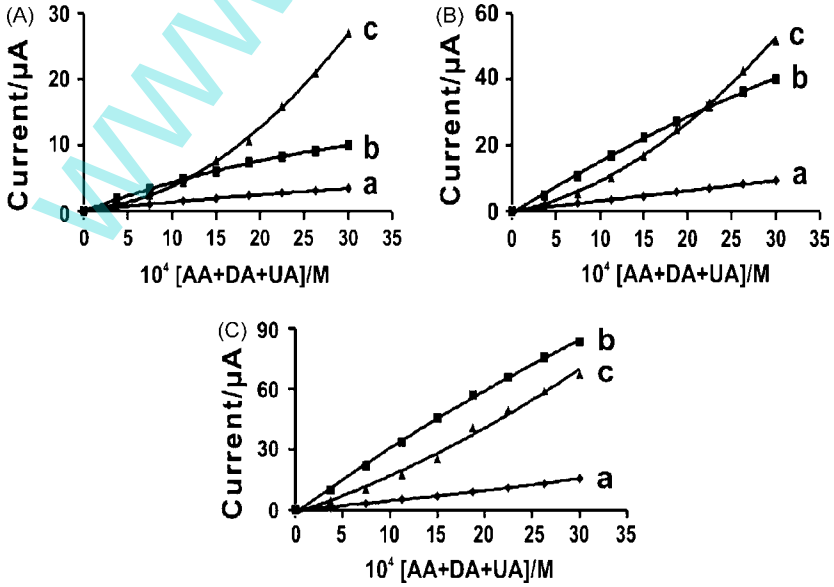

Fig. 7. (A); (B) and (C) shows the plot of current vs. different individual concentrations of AA, DA and UA mixture at composite-1, composite-2 and composite-3 films, respectively with: (a) AA; (b) DA and (c) UA, this shows the obvious increase in the activity of DA when increasing *f*-MWCNTs concentration.

values from the insets in Fig. 8 (A) and (C), revealed that in an AADAUA mixture, increasing concentration of AADAUA by each addition will decreases the increasing peak current rate of DA at about 106.75 μA for 1 μM^{-1} AA. But for UA, there was an increase in the increasing peak current rate at about 106.67 μA for 1 μM^{-1} AA. However, these changes were not visible from DPV waves. From these above DPV results, we conclude that composite-3 was suitable for the simultaneous detection of AA, DA and UA using DPV technique.

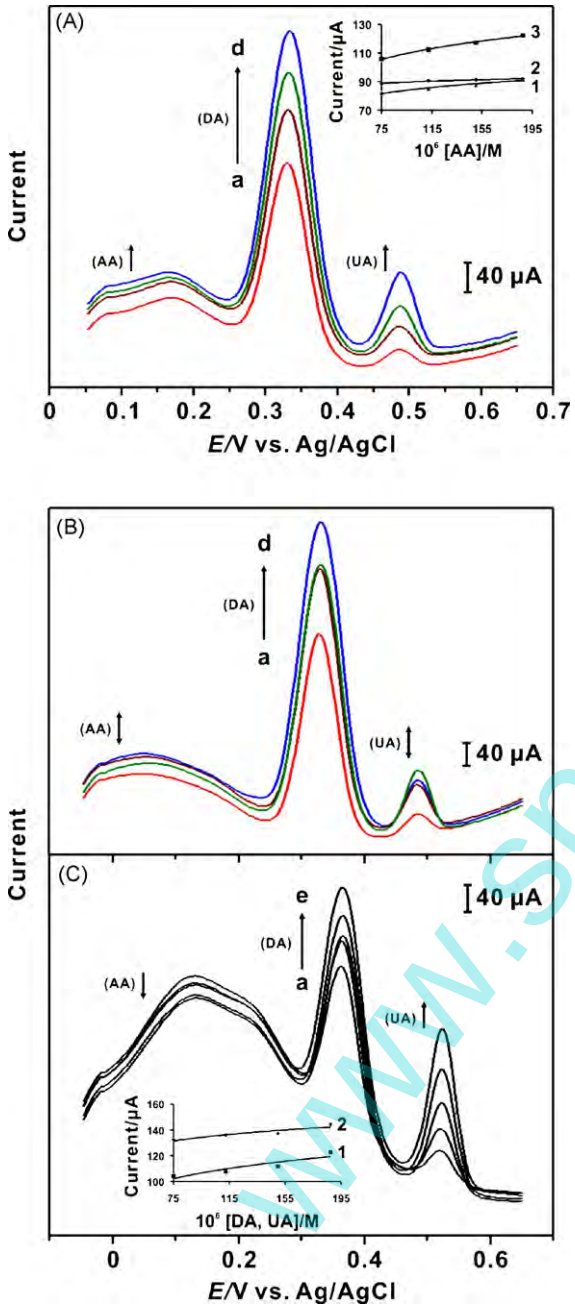

Fig. 8. DPVs of the (A) composite-3 film and (B) only *f*-MWCNTs in 0.1 M KHP buffer pH 4.0 aqueous solution with various individual concentrations of AA, DA and UA in a mixture: (a) 7.5×10^{-5}; (b) 1.125×10^{-4}; (c) 1.5×10^{-4} and (d) 1.875×10^{-4} M. Comparison of (A) and (B) shows the interference of three analytes between each other were higher in only *f*-MWCNTs modified GC. The inset in (A) shows the plot of current vs. different concentration of (1) UA; (2) AA and (3) DA in a mixture. (C) DPVs of composite-3 film at similar conditions with AA = 2×10^{-2} M and various individual concentrations of DA and UA in a mixture: (a) 7.5×10^{-5}; (b) 1.125×10^{-4}; (c) 1.5×10^{-4}; (d) 1.875×10^{-4} and (e) 2.25×10^{-4} M; in this AA peak current decreases when increasing DA and UA concentration. The inset in (C) shows the plot of current vs. different concentration of (1) UA and (2) DA in a mixture.

4. Conclusions

In conclusion, we have developed a novel composite material composed of functionalized MWCNTs with conjugated polymer (*f*-MWCNTs-PNR) on the GC, gold and ITO electrode surface using aqueous solutions. The EQCM confirmed the incorporation of PNR on the *f*-MWCNTs modified GC. The SEM and AFM results confirmed the difference between PNR and *f*-MWCNTs-PNR composite films morphological data. The *f*-MWCNTs-PNR composite film had excellent functional properties with good catalytic activity on a biochemical compounds such as AA, DA and UA. A detail study about the role of MWCNTs and its concentration effect on Epa and Ipa has been reported. The experimental method of CV and DPV with composite film biosensor integrated into a GC presented in this paper provides an opportunity for qualitative, quantitative characterization and simultaneous determination of AA, DA and UA at physiologically relevant conditions. Moreover, the DPV showed that the oxidation current of all three analytes was not affected by their coexistence in high concentrations. At the same time, the oxidized electrodes alleviate fouling problems, good repeatability of the voltammograms and stability. Therefore, this work establishes and illustrates, in principle and potential, a simple and novel approach for the development of a simultaneous AA, DA and UA voltammetric sensor, which is based on the modified GC, ITO and Au electrodes.

Acknowledgement

This work was supported by the National Science Council of the Taiwan (ROC).

References

[1] H.B. Mark Jr., J.F. Rubinson, J. Krotine, W. Vaughn, M. Goldschmidt, Electrochim. Acta 45 (2000) 4309.
[2] O. El Mouahid, C. Coutanceau, E.M. Belgsir, P. Crouigneau, J.M. Léger, C. Lamy, J. Electroanal. Chem. 426 (1997) 117.
[3] I. Becerik, F. Kadirgan, Synth. Met. 124 (2001) 379.
[4] S.M. Chen, Y.H. Fa, J. Electroanal. Chem. 553 (2003) 63.
[5] W. Zhang, F. Wan, W. Zhu, H. Xu, X. Ye, R. Cheng, L.T. Jin, J. Chromatogr. B. 818 (2005) 227.
[6] K. Gong, Y. Dong, S. Xiong, Y. Chen, L. Mao, Biosens. Bioelectron. 20 (2004) 253.
[7] L. Zhao, H. Liu, N. Hu, J. Colloid Interface Sci. 296 (2006) 204.
[8] R.P. Deo, J. Wang, Electrochem. Commun. 6 (2004) 284.
[9] M. Musameh, J. Wang, A. Merkoci, Y. Lin, Electrochem. Commun. 4 (2002) 743.
[10] J. Chen, J. Bao, C. Cai, T. Lu, Anal. Chim. Acta 516 (2004) 29.
[11] F.H. Wu, G.C. Zhao, X.W. Wei, Electrochem. Commun. 4 (2002) 690.
[12] L. Qian, X. Yang, Talanta 68 (2006) 721.
[13] G. Wu, Y.S. Chen, B.Q. Xu, Electrochem. Commun. 7 (2005) 1237.
[14] J. Wang, M. Musameh, Anal. Chim. Acta 511 (2004) 33.
[15] J. Wang, M. Li, Z. Shi, N. Li, Z. Gu, Electrochim. Acta 47 (2001) 651.

[16] Y. Yan, M. Zhang, K. Gong, L. Su, Z. Guo, L. Mao, Chem. Mater. 17 (2005) 3457.
[17] L. Qian, X. Yang, Electrochem. Commun. 7 (2005) 547.
[18] Q. Zhang, S. Rastogi, D. Chen, D. Lippits, P.J. Lemstra, Carbon 44 (2006) 778.
[19] Q. Li, J. Zhang, H. Yan, M. He, Z. Liu, Carbon 42 (2004) 287.
[20] J. Zhang, J.K. Lee, Y. Wu, R.W. Murray, Nano Lett. 3 (2003) 403.
[21] A. Star, T.R. Han, J. Christophe, P. Gabriel, K. Bradley, G. Gruner, Nano Lett. 3 (2003) 1421.
[22] M. Zhang, K. Gong, H. Zhang, L. Mao, Biosens. Bioelectron. 20 (2005) 1270.
[23] R.J. Chen, Y. Zhang, D. Wang, H. Dai, J. Am. Chem. Soc. 123 (2001) 3838.
[24] G. Han, J. Yuan, G. Shi, F. Wei, Thin Solid Films 474 (2005) 64.
[25] G.H. Deng, X. Xiao, J.H. Chen, X.B. Zeng, D.L. He, Y.F. Kuang, Carbon 43 (2005) 1557 (Letter to the Editor).
[26] E. Frackowiak, V. Khomenko, K. Jurewicz, K. Lota, F. Béguin, J. Power Sources 153 (2006) 413.
[27] B. Jill venton, R.M. Wightman, Anal. Chem. 1 (2003) 414A.
[28] G.F. Combs, The Vitamins: Fundamental Aspects in Nutrition and Health, second ed., Academic Press, San Diego, CA, 1992.
[29] P.J. O'Connell, C. Gormally, M. Pravda, G.G. Guilbault, Anal. Chim. Acta 431 (2001) 239.
[30] P. Capella, B. Ghasemzadech, K. Mitchekk, R.N. Adams, Electroanalysis 2 (1990) 175.
[31] G. Dryhurst, Electrochemistry of Biological Molecules, Academic Press, New York, 1977.
[32] J.M. Zen, J.J. Jou, G. Ilangovan, Analyst 123 (1998) 1345.
[33] J. Chen, C.S. Cha, J. Electroanal. Chem. 463 (1999) 93.
[34] M.A. Dayton, A.G. Ewing, R.M. Wightman, Anal. Chem. 52 (1980) 2392.
[35] P. Ramesh, G.S. Suresh, S. Sampath, J. Electroanal. Chem. 561 (2004) 173.
[36] A. Domenech, H. Garcia, M.T. Domenech-Carbo, M.S. Galletero, Anal. Chem. 74 (2002) 562.
[37] Y. Sun, B. Ye, W. Zhang, X. Zhou, Anal. Chim. Acta 363 (1998) 75.
[38] J. Premkumar, S.B. Khoo, J. Electroanal., Chem. 576 (2005) 105.
[39] S.M. Chen, K.C. Lin, J. Electroanal, Chem. 511 (2001) 101.
[40] C. Yang, J. Yi, X. Tang, G. Zhou, Y. Zeng, React. Func. Polym. 66 (2006) 1336.
[41] E. Laviron, J. Electroanal. Chem. 101 (1979) 19.
[42] G. Inzelt, E. CsahoÂk, Electroanalysis 11 (1999) 744.
[43] F. Vicente, J.J. García-Jareño, D. Benito, J. Agrisuelas, J. New Mat. Electrochem. Syst. 6 (2003) 267.
[44] S.M. Chen, M.I. Liu, Electrochim. Acta 51 (2006) 4744.
[45] S.M. Chen, C.J. Liao, V.S. Vasantha, J. Electroanal. Chem. 589 (2006) 15.
[46] J. Wang, J. Dai, T. Yarlagadda, Langmuir 21 (2005) 9.
[47] M. Tahhan, V.T. Truong, G.M. Spinks, G. GWallace, Smart Mater. Struct. 12 (2003) 626.
[48] F. Malem, D. Mandler, Anal. Chem. 65 (1993) 37.
[49] Y. Zhao, Y. Gao, D. Zhan, H. Liu, Q. Zhao, Y. Kou, Y. Shao, M. Li, Q. Zhuang, Z. Zhu, Talanta 66 (2005) 51.
[50] C. Hu, X. Chen, S. Hu, J. Electroanal. Chem. 586 (2006) 77.
[51] K. Wu, S. Hu, Microchim. Acta 144 (2004) 131.
[52] C.R. Raj, K. Tokuda, T. Ohsaka, Bioelectrochemistry 53 (2001) 183.
[53] A.A. Karyakin, E.E. Karyakina, H.L. Schmidt, Electroanalysis 11 (1999) 149.
[54] V.S. Vasantha, S.M. Chen, J. Electroanal. Chem. 592 (2006) 77.